Decentralized Control Design for Welding Mobile Manipulator

Tan Tung Phan*, Tan Lam Chung, Manh Dung Ngo,
Hak Kyeong Kim, Sang Bong Kim
Department of Mechanical Engineering,
College of Engineering, Pukyong National University,
San 100, Yongdang-Dong, Nam-Gu, Pusan 608-739, Korea

This paper presents a decentralized motion control method of welding mobile manipulators which use for welding in many industrial fields. Major requirements of welding robots are accuracy, robust, and reliability so that they can substitute for the welders in hazardous and worse environment. To do this, the manipulator has to take the torch tracking along a welding trajectory with a constant velocity and a constant heading angle, and the mobile-platform has to move to avoid the singularities of the manipulator. In this paper, we develop a kinematic model of the mobile-platform and the manipulator as two separate subsystems. With the idea that the manipulator can avoid the singularities by keeping its initial configuration in the welding process, the redundancy problem of system is solved by introducing the platform mobility to realize this idea. Two controllers for the mobile-platform and the manipulator were designed, respectively, and the relationships between two controllers are the velocities of two subsystems. Control laws are obtained based on the Lyapunov function to ensure the asymptotical stability of the system. The simulation and experimental results show the effectiveness of the proposed controllers.

Key Words : Decentralized Motion Control Method, Mobile Manipulator, Welding Reference Trajectory

Nomenclature

b : Distance between driving wheel and symmetry axis

e : Tracking error

J : Jacobian matrix

k : Positive constant

L_i : Length of ith link

^1p_E : Position vector of the end-effector with respect to the local frame

r : Radius of the wheel

$^0Rot_1$: Rotation transform matrix from the local frame to the world frame

^0V_E : Velocity vector of the end-effector with respect to the world frame

^1V_E : Velocity vector of the end-effector with respect to the local frame

^0V_P : Velocity vector of the center point of the mobile-platform with respect to the world frame

$(X\text{-}Y)$: The world coordinate system

$(x\text{-}y)$: The local coordinate system

Greeks

θ_i : Angle value of ith revolute joint

$\dot{\theta}_i$: Angular velocity of ith revolute joint

ω_{lw}, ω_{rw} : Angular velocities of left and right wheels

$^0\omega_P$: Rotational velocity of the local frame, i.e. the rotational velocity of the mobile-platform

* Corresponding Author,
E-mail : kimsb@pknu.ac.kr
TEL : +82-51-620-1606; **FAX :** +82-51-621-1411
Department of Mechanical Engineering, College of Engineering, Pukyong National University, San 100, Yongdang-Dong, Nam-Gu, Pusan 608-739, Korea.
(Manuscript **Received** April 2, 2004; **Revised** January 10, 2004)

Subscripts

1, 2, 3: Index of the joint 1, 2, 3

E, P : Index of the end-effector and the center
point of the mobile-platform

Superscripts

0, 1　: Index of the world coordinates system and
the local coordinate system

1. Introduction

Nowadays, welding robots become widely used in tasks which are harmful and dangerous for the welders. When a welding mobile robot moves along a welding trajectory, its sensors detect the errors, and its controller controls the torch so that it tracks correctly to a welding point on the welding trajectory i.e., the errors converge to zero. There are many types of welding robots such as wheeled mobile robots with slider, gantry manipulators, tracked manipulators, compound manipulators, and wheeled mobile manipulators. This paper deals with the wheeled mobile manipulator because it has a large working area. Traditional applications of manipulators involve accomplishing tasks within fixed workspaces. The stationary of the platform determines a static area within which the task must be structured so that the manipulator can execute the task efficiently. The effective workspace can be augmented by placing the manipulator on a mobile-platform.

In this study, we consider a mobile manipulator that consists of a three-linked manipulator mounted at the center point of a two-wheeled mobile-platform. We assume that the mobile-platform and the manipulator move at low speed because the welding velocity is just about 7.5 mm/s hence we ignore the inertia and the slipping between the wheels and the floor, so we only consider the kinematic representation for the mobile manipulator. We consider a mobile manipulator task, that is, the end-effector of the mobile manipulator tracks along a reference trajectory with a constant velocity and a constant heading angle. This manipulator moves in a horizontal plane, therefore, we apply the motion law of rigid body in a plane to define the velocity of

the end-effector with respect to the world frame. The velocity of the end-effector (also the velocity of torch) must keep up the welding velocity in the whole welding process.

The mobile manipulator is a topic that has been studied by many researchers in recent years. Yoo et al.(2001) developed a control algorithm for a three-linked welding mobile manipulator like the one in this study based on the Lagrange's equations of motion. They used laser range sensors to guide the mobile-platform, and a vision sensor to guide the end-effector of the manipulator. Seraji (1995) developed a simple on-line coordinated control of mobile robot, and the redundancy problem is solved by introducing a set of user-specified additional task during the end-effector motion. He defined a scalar cost function and minimized it to have no singularity. Yamamoto and Yun (1994) developed a control algorithm for the mobile-platform so that the manipulator is always positioned at the preferred configurations measured by its manipulability to avoid the singularity. Jeon et al. (2002) applied the two-wheeled mobile robot with a torch slider for welding automation. They proposed a seam-tracking and motion control of the welding mobile robot for lattice-type welding. Bui et al.(2003) proposed an adaptive tracking control method base on the Lyapunov function to enhance the tracking properties of a two wheeled welding mobile robot.

The wheeled mobile-platform is subject to nonholonomic constraints while the manipulator is usually unconstrained, hence we choose the mobile manipulator to perform the welding task because it has faster response than the wheeled mobile-platform with the torch fixed or slider. The mobile manipulator has five DOF-three DOF of manipulator and two DOF of mobile-platform-whereas the welding task requires only three DOF. Hence, the mobile manipulator is a kinematic redundant system. To solve this problem, we added two constraints that are linear and rotational velocities of mobile-platform. This means that the mobile-platform motion is not a free motion but it is a constrained motion. The target of two constraints is to avoid the

singularity of the manipulator by keeping the initial configuration of manipulator.

In this paper we develop a kinematic representation for the mobile manipulator in which the mobile manipulator is treated as two separate subsystems rather than treating as a single entity in the method of Seraji (1995). A decentralized motion control method is developed to control this complicated system. Every subsystem has one controller and the relations among the controllers are the velocities of subsystems. This method is more flexible than the centralized motion control method that uses a single controller to control entire system because the controllers are independent. Therefore it is simple and easy to design them. We propose two controllers, one for the manipulator and another for the mobile-platform, based on the Lyapunov control function to enhance the tracking properties of the mobile manipulator.

The mobile-manipulator prototype is shown in Fig. 1. We use three DC motors to drive three revolute joints of the manipulator, and two DC motors to drive two wheels of the mobile-platform. The torch mounted on the third-link of the manipulator and the touch sensor also mounted on the third-link, but its position is above the torch. The touch sensor touches and rolls along a steel wall to detect the tracking errors.

Finally, the simulation results on computer and the experimental results are presented to show the effectiveness of the proposed method.
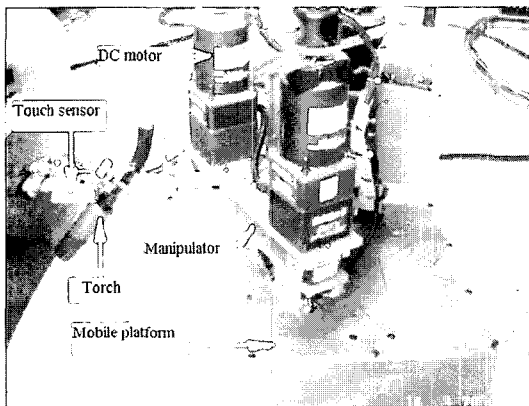

Fig. 1   The mobile-manipulator prototype

2. Kinematic Equations

2.1 Kinematic equations of the manipulator

We consider a three-linked manipulator as in Fig. 2. We attach a Cartesian coordinate frame at the center point of the mobile-platform. Because this frame is fixed to the mobile-platform and moves in the world frame therefore this frame is called the local frame.

Let us denote $^1V_E = [^1\dot{x}_E\ ^1\dot{y}_E\ ^1\dot{\phi}_E]^T$ is the velocity vector of the end-effector with respect to the local frame and $\dot{\theta} = [\dot{\theta}_1\ \dot{\theta}_2\ \dot{\theta}_3]^T$ is the angular velocity vector of the joint angle. The velocity vector of the end-effector with respect to the local frame is determined as

$$^1V_E = J\dot{\theta} \qquad (1)$$

where

$$J = \begin{bmatrix} -L_3S_{123}-L_2S_{12}-L_1S_1 & -L_3S_{123}-L_2S_{12} & -L_3S_{123} \\ L_3C_{123}+L_2C_{12}+L_1C_1 & L_3C_{123}+L_2C_{12} & L_3C_{123} \\ 1 & 1 & 1 \end{bmatrix}$$

$S_1 = \sin(\theta_1);\ S_{12} = \sin(\theta_1+\theta_2);\ S_{123} = \sin(\theta_1+\theta_2+\theta_3)$

$C_1 = \cos(\theta_1);\ C_{12} = \cos(\theta_1+\theta_2);\ C_{123} = \cos(\theta_1+\theta_2+\theta_3)$

Let us denote $^0V_E = [^0\dot{x}_E\ ^0\dot{y}_E\ ^0\dot{\phi}_E]^T$ is the velocity vector of the end-effector with respect to the
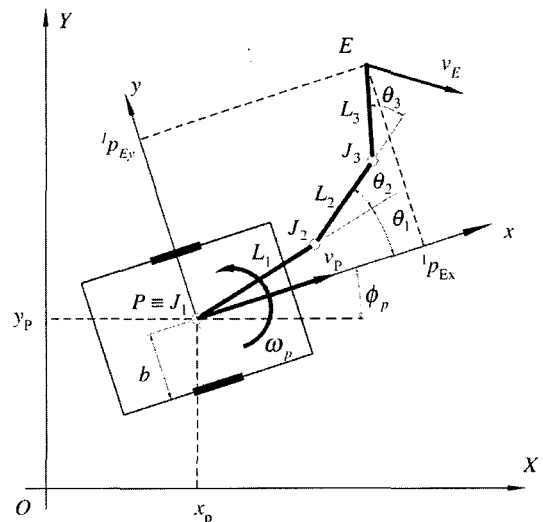

Fig. 2   Scheme for deriving the mobile manipulator kinematic equations

world frame. This velocity can be obtained from the motion equation of a rigid body in a plane as follows

$$^0V_E = {}^0V_P + {}^0W_P \times {}^0Rot_1 {}^1p_E + {}^0Rot_1 {}^1V_E \quad (2)$$

where $^0V_P = [\dot{x}_P \ \dot{y}_P \ 0]^T$ is the linear velocity vector of the mobile-platform with respect to the world frame, $^0W_P = [0 \ 0 \ \omega_P]^T$ is the rotational velocity vector of the mobile-platform with respect to the world frame, $^1p_E = [L_1S_1 + L_2S_{12} + L_3 S_{123} \ L_1C_1 + L_2C_{12} + L_3C_{123} \ 1]^T$ is the position vector of the end-effector with respect to the local frame and the rotation transform matrix from the local frame to the world frame is given by

$$^0Rot_1 = \begin{bmatrix} \cos \phi_P & -\sin \phi_P & 0 \\ \sin \phi_P & \cos \phi_P & 0 \\ 0 & 0 & 1 \end{bmatrix}$$

2.2 Kinematic equations of the mobile-platform

We consider a two-wheeled mobile-platform as in Fig. 2. When the mobile-platform moves in the horizontal plane, it obtains the linear velocity v_p, and the angular velocity ω_p. The relationship between v_p, ω_p and the angular velocities of the two driving wheels is given by

$$\begin{bmatrix} \omega_{rw} \\ \omega_{lw} \end{bmatrix} = \begin{bmatrix} 1/r & b/r \\ 1/r & -b/r \end{bmatrix} \begin{bmatrix} v_p \\ \omega_p \end{bmatrix} \quad (3)$$

where ω_{rw}, ω_{lw} are the angular velocities of the right and left wheels.

3. Controllers Design

3.1 Controller design for the manipulator

We assume that the wheels roll and avoid slipping. The coordinate relations of the mobile manipulator with the reference welding path are shown in Fig. 3. Our objective is to design controller so that the end-effector which has coordinates $E(x_E \ y_E \ \phi_E)$ tracks to the reference point $R(x_R \ y_R \ \phi_R)$. We define the tracking error vector $E_E = [e_1 \ e_2 \ e_3]^T$ as follows

$$\begin{bmatrix} e_1 \\ e_2 \\ e_3 \end{bmatrix} = \begin{bmatrix} \cos \phi_E & \sin \phi_E & 0 \\ -\sin \phi_E & \cos \phi_E & 0 \\ 0 & 0 & 1 \end{bmatrix} \begin{bmatrix} x_R - x_E \\ y_R - y_E \\ \phi_R - \phi_E \end{bmatrix} \quad (4)$$
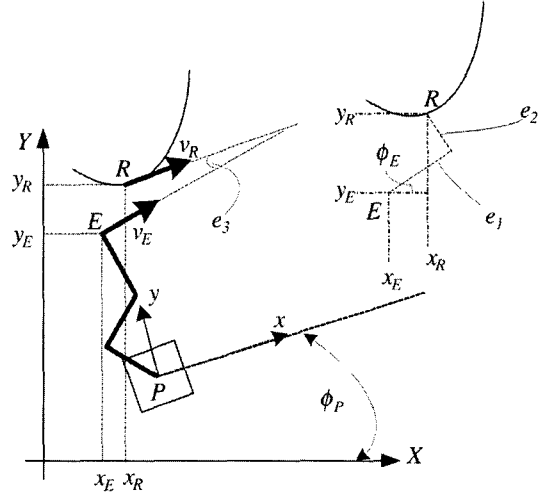

Fig. 3 Scheme for deriving the error equations of manipulator

Let us denote

$$A = \begin{bmatrix} \cos \phi_E & \sin \phi_E & 0 \\ -\sin \phi_E & \cos \phi_E & 0 \\ 0 & 0 & 1 \end{bmatrix}$$

$$B = [x_R - x_E \ y_R - y_E \ \phi_R - \phi_E]^T$$

We can re-express Eq. (4) as follows:

$$E_E = A \ B \quad (5)$$

We will design a controller to achieve $e_i \to 0$ when $t \to \infty$, and hence the end-effector tracks to its reference point R. The derivative of Eq. (4) is given by

$$\begin{bmatrix} \dot{e}_1 \\ \dot{e}_2 \\ \dot{e}_4 \end{bmatrix} = \omega_E \begin{bmatrix} -\sin \phi_E & \cos \phi_E & 0 \\ -\cos \phi_E & -\sin \phi_E & 0 \\ 0 & 0 & 0 \end{bmatrix} \begin{bmatrix} x_R - x_E \\ y_R - y_E \\ \phi_R - \phi_E \end{bmatrix}$$
$$+ \begin{bmatrix} \cos \phi_E & \sin \phi_E & 0 \\ -\sin \phi_E & \cos \phi_E & 0 \\ 0 & 0 & 1 \end{bmatrix} \begin{bmatrix} \dot{x}_R - \dot{x}_E \\ \dot{y}_R - \dot{y}_E \\ \dot{\phi}_R - \dot{\phi}_E \end{bmatrix} \quad (6)$$

Let us denote $V_R = [\dot{x}_R \ \dot{y}_R \ \dot{\phi}_R]^{T'}$ is the velocity vector of the welding reference point and

$$C = \begin{bmatrix} -\sin \phi_E & \cos \phi_E & 0 \\ -\cos \phi_E & -\sin \phi_E & 0 \\ 0 & 0 & 0 \end{bmatrix}$$

Now, we re-express Eq. (6) as follows

$$\dot{E}_E = \omega_E C \ B + A(V_R - {}^0V_E) \quad (7)$$

The Lyapunov function is chosen as

$$V_0 = \frac{1}{2} e_1^2 + \frac{1}{2} e_2^2 + \frac{1}{2} e_3^2 \qquad (8)$$

and its derivative is

$$\dot{V}_0 = e_1\dot{e}_1 + e_2\dot{e}_2 + e_3\dot{e}_3 \qquad (9)$$

To achieve the negative of $\dot{V}_0$ the following equation must be satisfied

$$\dot{E}_E = -K\,E_E \qquad (10)$$

where $K = \mathrm{diag}(k_1, k_2, k_3)$ with k_1, k_2, k_3 are the positive values.

We substitute Eqs. (1), (2), (10) into Eq. (7), we obtain Eq. (11) as follows

$$-K\,E_E = \omega_E C\,B + A(V_R - ({}^0V_P + {}^0W_P \\ \times {}^0Rot_1\,{}^1p_E + {}^0Rot_1\,J\,\dot{\theta})) \qquad (11)$$

The errors e_1, e_2, e_3 converge to zero when the angular velocity vector of the joint satisfies the control law as

$$\theta = J^{-1}\,{}^0Rot_1^{-1}(A^{-1}(\omega_E C\,B + K\,E_E) \\ + V_R - {}^0V_P - {}^0W_P \times {}^0Rot_1\,{}^1p_E) \qquad (12)$$

Eq. (12) is the controller for the manipulator, and it can be re-expressed as

$$\dot{\theta}_1 = \frac{1}{L_1 S_2}\left(\begin{matrix} v_R S_{3e_3} - v_P C_{12} + (e_2 k_2 - e_1\omega_E) C_3 \\ -(e_1 k_1 + e_2\omega_E + L_3(\omega_R + e_3(k_3 + \omega_E))) S_3 \end{matrix} \right) - \omega_P \qquad (13a)$$

$$\dot{\theta}_2 = \frac{1}{L_1 L_2 S_2}\left| \begin{matrix} -v_R(L_1 S_{23e_3} + L_2 S_{3e_3}) + v_P(L_1 C_1 + L_2 C_{12}) \\ +(\omega_E e_1 - e_2 k_2)(L_1 C_{23} + L_2 C_3) \\ -(L_1 S_{12} + L_2 S_2)(L_3 e_3(k_3 + \omega_E) + L_3\omega_R + e_1 k_1 + e_2\omega_E) \end{matrix} \right| (13b)$$

$$\dot{\theta}_3 = \frac{1}{L_2 S_2}\left(\begin{matrix} (e_2\omega_E + k_1 e_1 + L_3(\omega_R + e_3(k_3 + \omega_E))) S_{23} \\ +(e_2 k_2 - e_1\omega_E) C_{23} + v_R S_{23e_3} - v_P C_1 \end{matrix} \right) \\ + (\omega_R + e_3(k_3 + \omega_E)) \qquad (13c)$$

where $S_{23e_3} = \sin(\theta_2 + \theta_3 + e_3)$ and $S_{3e_3} = \sin(\theta_3 + e_3)$.

3.2 Controller design for the mobile-platform

The task of the mobile-platform is to move to avoid the singularity of the configuration of the manipulator. We propose a simple algorithm for the mobile-platform to avoid the singularity by keeping its initial configuration in the whole welding process.
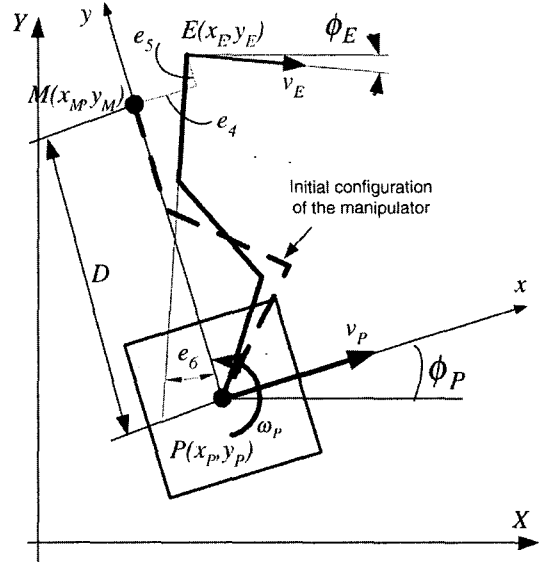

Fig. 4 Scheme for deriving the kinematic equations of mobile-platform

We choose the initial configuration of the manipulator as in Fig. 4. Let us denote a point $M(x_M, y_M, \phi_M)$ which is a fixed point with respect to the local frame. This point coincides with the point E of the end-effector at beginning.

In order to keep the configuration of the manipulator goes away from the singularity, the mobile-platform has to move so that the point M tracks to the point E. Consequently, the initial configuration of the manipulator is maintained in the whole welding process, and the singularity is not appeared.

From Fig. 4, we get the geometric relations as

$$\begin{aligned} x_M &= x_P - D\sin\phi_P \\ y_M &= y_P + D\cos\phi_P \\ \phi_M &= \phi_P \end{aligned} \qquad (14)$$

Hence, we have

$$\begin{aligned} \dot{x}_M &= v_P\cos\phi_P - D\omega_P\cos\phi_P \\ \dot{y}_M &= v_P\sin\phi_P - D\omega_P\sin\phi_P \\ \dot{\phi}_M &= \dot{\phi}_P \end{aligned} \qquad (15)$$

Our objective is to design controller so that the point $M(x_M, y_M, \phi_M)$ tracks to the end-effector $E(x_E\ y_E\ \phi_E)$. We define the tracking errors $[e_2\ e_5\ e_6]^T$ as follows

$$\begin{bmatrix} e_4 \\ e_5 \\ e_6 \end{bmatrix} = \begin{bmatrix} \cos \phi_M & \sin \phi_M & 0 \\ -\sin \phi_M & \cos \phi_M & 0 \\ 0 & 0 & 1 \end{bmatrix} \begin{bmatrix} x_E - x_M \\ y_E - y_M \\ \phi_E - \phi_M \end{bmatrix} \quad (16)$$

Differentiate Eq. (16) and substitute Eq. (14) and (15) into (16) we have

$$\begin{bmatrix} \dot{e}_4 \\ \dot{e}_5 \\ \dot{e}_6 \end{bmatrix} = \begin{bmatrix} v_E \cos e_6 \\ v_E \sin e_6 \\ \omega_E \end{bmatrix} + \begin{bmatrix} -1 & e_5 + D \\ 0 & -e_4 \\ 0 & -1 \end{bmatrix} \begin{bmatrix} v_P \\ \omega_P \end{bmatrix} \quad (17)$$

The chosen Lyapunov function and its derivative are given as

$$V_0 = \frac{1}{2} e_4^2 + \frac{1}{2} e_5^2 + \frac{1 - \cos e_6}{k_5} \quad (18)$$

$$\dot{V}_0 = e_4 \dot{e}_4 + e_5 \dot{e}_5 + \frac{\sin e_6}{k_5} \dot{e}_6 \quad (19)$$

$$\dot{V}_5 = e_4 (v_P + D\omega_P + v_E \cos e_6) \\ + \frac{\sin e_6}{k_5} (-\omega_P + \omega_E + k_5 e_5 v_E) \quad (20)$$

An obvious way to achieve negative of V_0 is to choose (v_P, ω_P) as

$$v_P = D(\omega_E + k_5 e_5 v_E + k_6 \sin e_6) \\ + v_E \cos e_6 - k_4 e_4 \quad (21)$$

$$\omega_P = \omega_E + k_5 e_5 v_E + k_6 \sin e_6 \quad (22)$$

where k_4, k_5 are k_6 positive values.

4. Measurement of the Errors

4.1 Measurement of the errors e_1, e_2, e_3

In order to measure the tracking error components e_1, e_2, e_3, we propose a simple measurement scheme using potentiometers as in Fig. 6. Two rollers are placed at points O_2 and O_3 .We need two sensors for measuring the errors, that is, one linear sensor for measuring d, and one rotating sensor for measuring the angle between the torch and the tangent line of the wall at the welding point.

From Fig. 6, we have the relation as follows

$$e_1 = r \sin e_3$$
$$e_2 = d + r |\cos e_3| \quad (23)$$
$$e_3 = \angle (O_1 O_3, O_1 E) - \pi/2$$

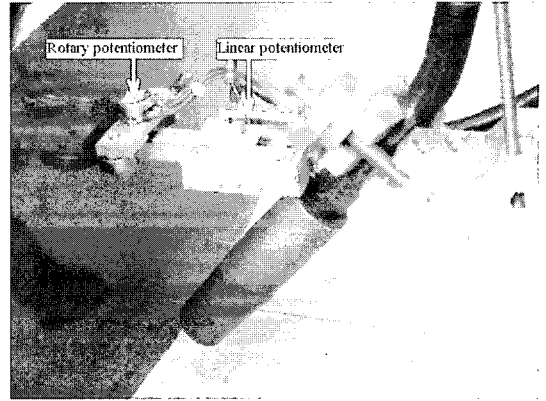where r is the radius of the roller, d is the length

Fig. 5 The touch sensor used in experiment
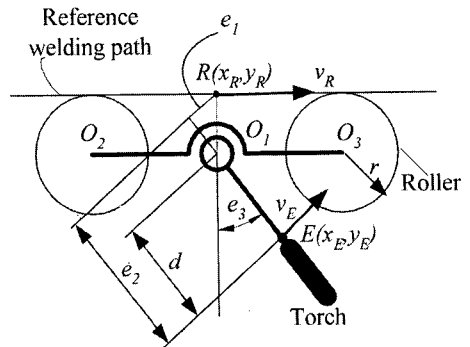

Fig. 6 Scheme of measuring the errors e_1, e_2, e_3

which is measured by the linear potentiometer, and e_3 is the angle which is measured by the rotating potentiometer. In Fig. 6, the welding path is a line ; if the welding path is a curve then Eq. (23) is also valid if we choose the distance O_2 O_3 enough small, and the radius of the welding path enough large.

4.2 Measurement of the errors e_4, e_5, e_6

From Fig. 4, the errors e_4, e_5, and e_6 can be calculated as

$$e_4 = {}^1x_E - {}^1x_M = L_1 \cos \theta_1 + L_2 \cos (\theta_1 + \theta_2) \\ + L_3 \cos (\theta_1 + \theta_2 + \theta_3)$$

$$e_5 = {}^1y_E = {}^1y_M = L_1 \sin \theta_1 + L_2 \sin (\theta_1 + \theta_2) \\ + L_3 \sin (\theta_1 + \theta_2 + \theta_3) - D \quad (24)$$

$$e_6 = {}^1\phi_E - \frac{\pi}{2} = (\theta_1 + \theta_2 + \theta_3) - \frac{\pi}{2}$$

The joint angles θ_1, θ_2 and θ_3 can be determined
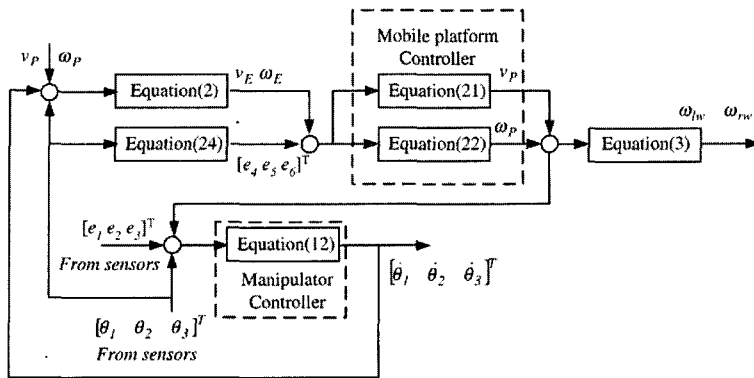
Fig. 7 Schematic diagram of applied method

from the rotary potentiometers which are assembled at the joints of the manipulator.

Fig. 7 shows the schematic diagram of kinematic system of the mobile-manipulator. The tracking errors e_1, e_2 and e_3 derive from the touch sensor (see Section 4.1), and the angle values derive from the rotary potentiometers. There are two controllers for two subsystems (hidden-line rectangular), and the relation between them are the velocities of two subsystems.

5. Simulation Results and Discussion

In this section, some simulation results are presented to demonstrate the effectiveness of the control algorithm developed for mobile manipulator. Table 1 shows the parameters and the initial values for the welding wheeled mobile manipulator system used in this simulation.

The reference welding path is chosen as in Fig. 8. From the simulation results, as in Fig. 9, we can find that the end-effector of the manipulator tracks to the welding point, and moves on the
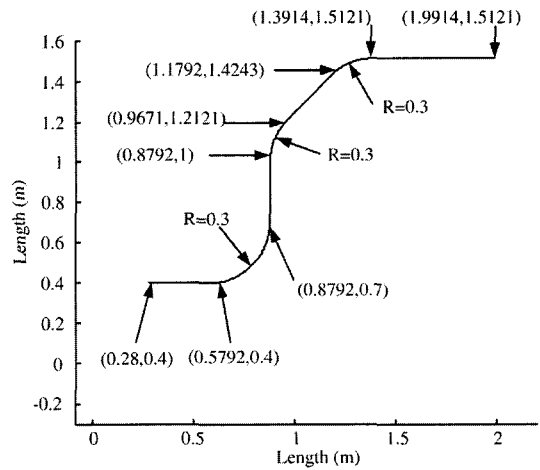
Fig. 8 Reference welding path

Table 1 The numerical values and initial values for simulation

Parameters	Values	Units	Parameters	Values	Units
b	0.105	M	x_E $(t=0)$	0.275	m
R	0.025	m	y_E $(t=0)$	0.395	m
L_1	0.2	m	ϕ_E $(t=0)$	-15	deg.
L_2	0.2	m	θ_1 $(t=0)$	135	deg.
L_3	0.2	m	ϕ_2 $(t=0)$	-90	deg.
k_1	1	—	θ_3 $(t=0)$	45	deg.
k_2	1.3	—	k_4	1	—
k_3	1.8	—	k_5	5000	—
v_R	0.0075	m/s	k_6	1	–

reference welding trajectory with a constant velocity. We also find that, the mobile manipulator moves to keep the initial configuration of the manipulator.

In this simulation, the controller for the manipulator is given by Eq. (12). For the mobile-platform, we use Eqs. (21), (22) as its controller.

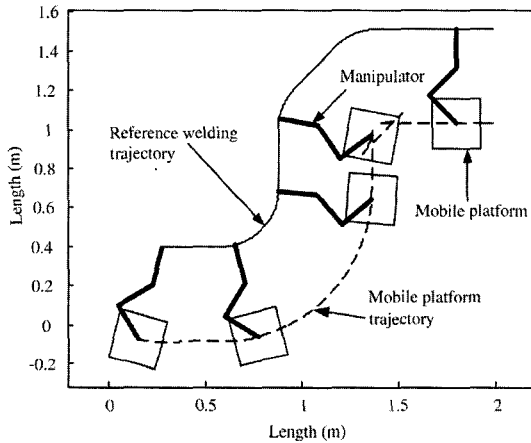Fig. 10 shows that, from the initial error values $e_1=4$ mm, $e_2=6$ mm ; $e_3=15°$, the errors e_1, e_2,

e_3 converge to zero after about 2.5 seconds. Fig. 11 shows the errors of the mobile-platform controller. This controller controls the mobile-platform to keep the initial configuration of the manipulator, therefore, the errors e_4, e_5, e_6 converge to zero more slowly than the tracking errors e_1, e_2, e_3. The errors e_4 e_5 e_6, however, do not need a fast convergence because they do not influence the quality of the welding path. In Fig. 12, we can see that the end-effector tracks to welding reference point when the errors exist. Fig. 13 shows the velocity of the end-effector attained
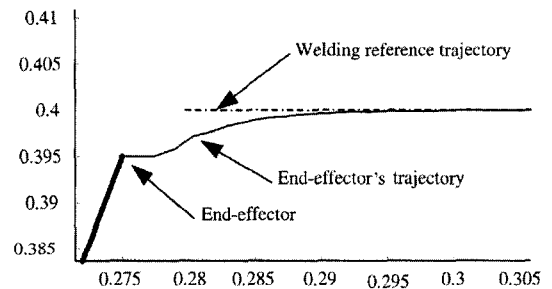

Fig. 9 The mobile manipulator tracks along the welding path

Fig. 12 Trajectory of the end-effector and its reference at beginning

Fig. 10 The tracking errors e_1, e_2, e_3 at beginning
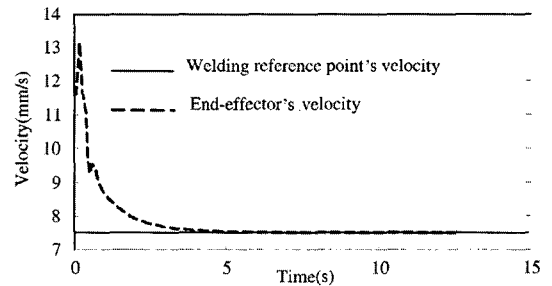
Fig. 13 The velocities of welding reference point and the end-effector at beginning

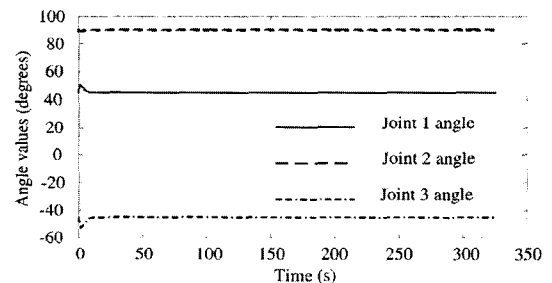Fig. 11 The tracking errors e_4, e_5, e_6 at beginning

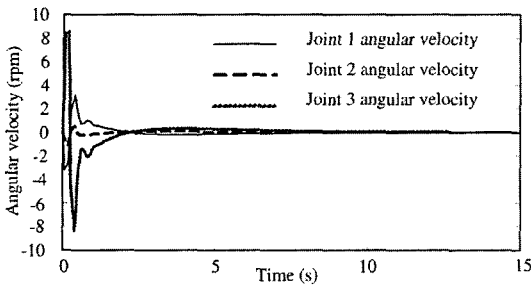Fig. 14 The angle values of three revolute joints

Fig. 15 The angular velocities of three revolute joints of manipulator at beginning
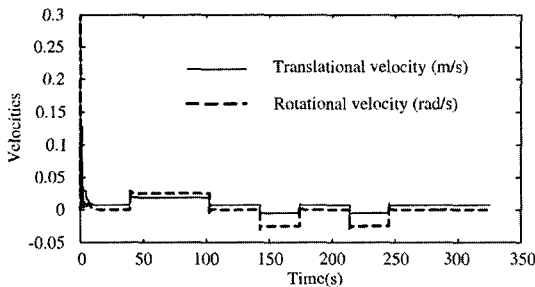

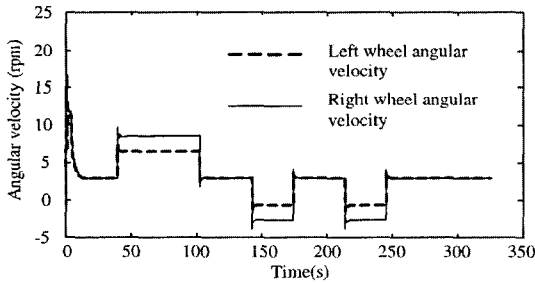**Fig. 16** The velocities of the mobile-platform

Fig. 17 The angular velocities of two wheels of the mobile-platform

the welding reference point velocity that is 7.5 mm/s when the errors equal to zero. The angle values of three revolute joints are given in Fig. 14. Fig. 15 shows the angular velocities of three joints. Fig. 16 shows the velocities of the mobile-platform and Fig. 17 shows the angular velocities of left and right wheels of the mobile-platform.

6. The Experimental Results

6.1 he configuration of the control system
The DSP-PIC based control system was de-

veloped for the mobile manipulator which can implement a complicated control law. The control system was modularized as function to perform special control.

The control system is based on the integration of two levels of controllers : device controller and master controller. The former is based on six PIC16F877 microprocessors of which one PIC16F877 has a function as interface between the two levels, and the others are left-wheel controller, right-wheel controller, joint-1 controller, joint-2 controller and joint-3 controller to drive the wheels and the joints, respectively ; the latter is based on TMS320C32 DSP processor which renders the control law and sends command to the device controller. The device controllers are DC motor drivers that perform indirectly servo control using one encoder. The two A/D ports on master controller are connected to the two potentiometers for sensing the errors, as mentioned in section 4.1, and the three others are connected to measure the angle of the link needed for the controller. The interface controller links to the servo controllers via I2C communication, and the interface controller, in turn, links to the master controller via RS232 communication. The entire configuration of the control system is shown in Fig. 18.

For operation, the master controller receives signals from sensors to achieve the errors by Eq. (23), the control law Eq. (12) and Eqs. (21), (22) are rendered based on the errors for the sampling time of 100 ms, and the velocity commands are sent to the five servo controllers, respectively. The parameters of the system, such as controller's constants, are set by display and keypad.

6.2 Experimental results
A welding mobile manipulator prototype has constructed to check the simulation results on computer. We use 5 DC motors (15W/24V) to drive 3 revolute joints and 2 wheels. Every DC motor has the encoder to measure its angular velocity, and every revolute joint has the rotary potentiometer to measure its joint angle value. Table 2 shows the parameters and the initial

values of the welding wheeled mobile manipulator used in this experiment.

In practice, the welding mobile manipulator can weld with the unknown trajectory in advance. The end-effector tracks to the welding trajectory by using the errors from the touch sensor. However, in order to compare with the simulation results the welding path in this experiment is chosen similar with the welding path in Fig.8.

The tracking errors of the manipulator e_1, e_2, e_3 and the tracking errors of the mobile-platform e_4, e_5, e_6 are recorded. They are shown from Fig. 20 to Fig. 25.

From the experiment result, we find that the tracking errors vibrate around their simulation values. These disturbances are consequence of several causes such as the backlash of the gear, the rough of the steel wall, disturbances from the

Table 2 The parameters and initial values in experiment

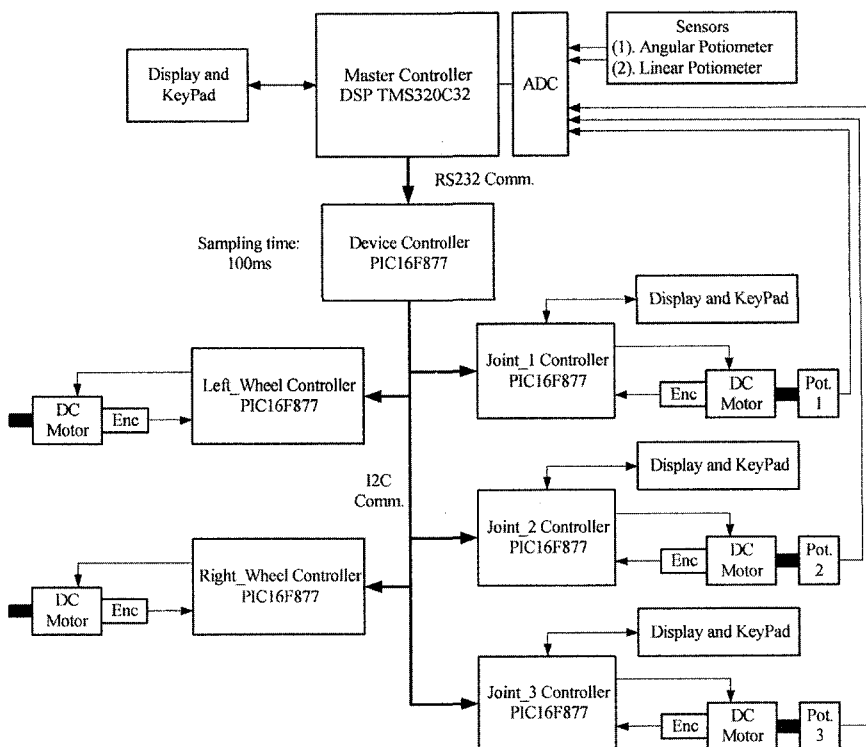| Parameters	Values	Units	Parameters	Values	Units
b	0.105	m	$x_R - x_E$ $(t=0)$	0.005	m
r	0.025	m	$y_R - y_E$ $(t=0)$	0.005	m
L_1	0.2	m	$\phi_R - \phi_E$ $(t=0)$	-15	deg.
L_2	0.2	m	θ_1 $(t=0)$	135	deg.
L_3	0.2	m	θ_2 $(t=0)$	-90	deg.
k_1	1	—	θ_3 $(t=0)$	45	deg.
k_2	1.3	—	k_4	1	—
k_3	1.8	—	k_5	5000	—
v_R	0.0075	m/s	k_6	1	—

Fig. 18 The configuration of the control system

electronic circuit etc. However, these vibrations have small amplitude, and they are not influenced enough to the welding process.

From the simulation and experimental results, we can conclude that the controllers can be applied for a welding mobile manipulator to weld a smooth curved path in the horizontal plane.
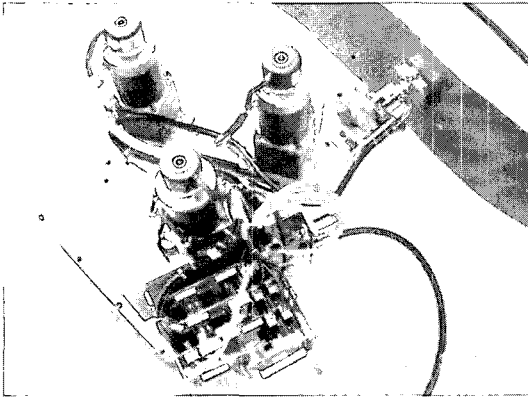

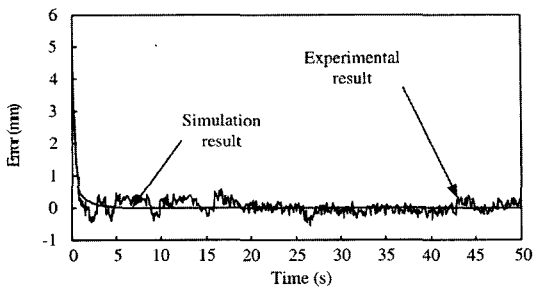**Fig. 19**   The welding mobile manipulator is tracking along the welding path in experiment

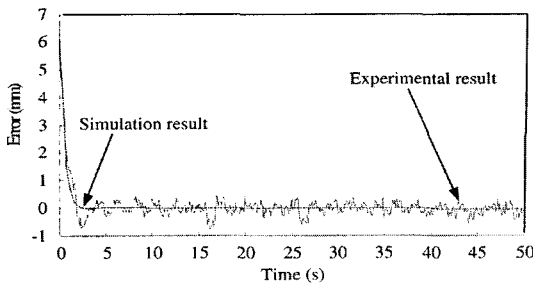**Fig. 20**   The tracking error e_1 from the simulation and experiment

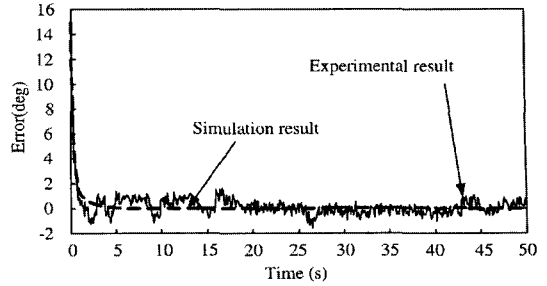**Fig. 21**   The tracking error e_2 from the simulation and experiment

Fig. 22   The tracking error e_3 from the simulation and experiment
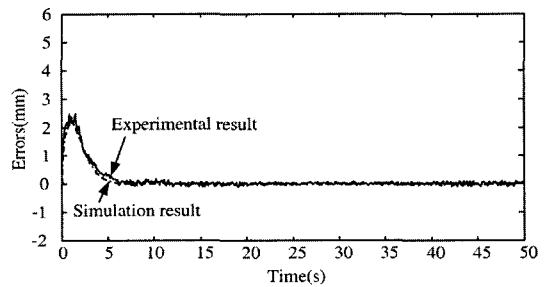

Fig. 23   The tracking error e_4 from the simulation and experiment
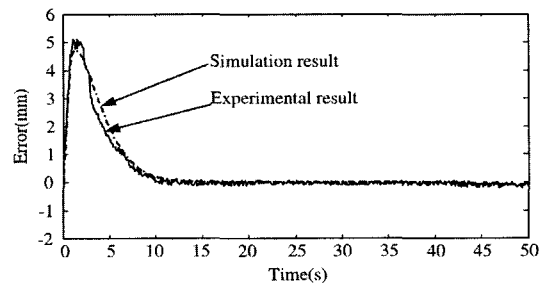

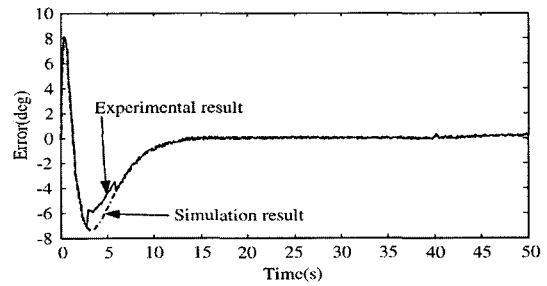**Fig. 24**   The tracking error e_5 from the simulation and experiment

Fig. 25   The tracking error e_6 from the simulation and experiment

7. Conclusions

This paper introduced the decentralized motion control method for the welding mobile manipulator. The controllers based on the Lyapunov control function to enhance the tracking stable properties of the mobile manipulator. The kinematic equations, which are constructed for each subsystem, are simpler than the kinematic equations for entire system. Two independent controllers are proposed to control two subsystems, and the relations between them are the velocities of subsystems of the previous sampling time. A simple path planning for the mobile-platform is proposed to avoid the singularity for the manipulator's configuration. The tracking errors of the end-effector can be measured by two simple sensors to derive the controller for the manipulator. The hardware, which is used to control the DC motors, are also designed to carry-out the experiment. The simulation results show that the controllers can be used for the mobile manipulators control with good performance. The experiment have been done with the mobile manipulator prototype to compare with the simulation results on computer. The experimental results also prove the effectiveness of the proposed controllers.

References

Bayle, B., Fourquet, I. Y., Lamiraux, F. and Renaud, M., 2002, "Kinematic Control of Wheeled Mobile Manipulators," *Proc. IEEE/RSJ International Conference on Intelligent Robots and Systems*, Vol. 2, pp. 1572~1577.

Bui, T. H., Chung, T. L. and Kim, S. B., 2003, "Adaptive Tracking Control of Two-Wheeled Welding Mobile Robot with Smooth Curved Welding Path," *KSME International Journal*, Vol. 17, No. 1, pp. 1682~1692.

Carriker, W. F., Khosla, P. K. and Krogh, B. H., 1990, "The Use of Simulated Annealing to Solve The Mobile Manipulator Path Planning Problem," *Proc. IEEE International Conference on Robotics and Automation*, pp. 204~209.

Hootsmans, N. A. M., and Dubowsky, S., 1991, "Large Motion Control of Mobile Manipulator Including Vehicle Suspension Characteristics," *Proc. IEEE International Conference on Robotics and Automation*, pp. 2336~2341.

Jeon, Y. B., Kam, B. O., Park, S. S. and Kim, S. B., 2002, "Modeling and Motion Control of Mobile Robot for Lattice Type Welding," *KSME International Journal*, Vol. 16, No. 1, pp. 83~93.

Kam, B. O., Jeon, Y. B., Suh, J. H., Oh, M. S. and Kim, S, B., 2003, "Motion Control of Two-Wheeled Mobile Robot with Seam Tracking Sensor," *International Journal of The Korean Society of Precision Engineering*, Vol. 4, No. 2, pp. 30~38.

Kanayama, Y., 1994, "Two Dimensional Wheeled Vehicle Kinematics," *Proc. IEEE International Conference*, Vol. 4, pp. 3079~3084.

Kerrow, Ph. J. Mc., 1991, *Introduction to Robotics*, Addison-Wesley Publishers, pp. 233~288.

Phan, T. T., Suh, J. H. and Kim, S. B., 2003, "Decentralized Motion Control of Mobile Manipulator," *Proc. ICCAS International Conference on Control, Automation and Systems*, pp. 1841~1846.

Seraji, H., 1995, "Configuration Control of Rover-Mounted Manipulators," *Proc. IEEE International Conference on Robotics and Automation*, Vol. 3, pp. 2261~2266.

Yamamoto, Y. and Yun, X., 1992, "Coordinating Locomotion and Manipulation of A Mobile Manipulator," *Proc. IEEE International Conference on Decision and Control*, pp. 2843~2848.

Yoo, W. S., Kim, J. D. and Na, S. J., 2001, "A Study on A Mobile-Platform Manipulator Welding System for Horizontal Fillet Joints," *Trans. Mechatronics*, Vol. 11, pp. 853~868.